Brain Structure and Function (2019) 224:471–483
https://doi.org/10.1007/s00429-018-1783-1

ORIGINAL ARTICLE

# Cortistatin-expressing interneurons require TrkB signaling to suppress neural hyper-excitability

Julia L. Hill[1] · Dennisse V. Jimenez[1] · Yishan Mai[1] · Ming Ren[1] · Henry L. Hallock[1] · Kristen R. Maynard[1] · Huei-Ying Chen[1] · Nicholas F. Hardy[1] · Robert J. Schloesser[2] · Brady J. Maher[1,3] · Feng Yang[1] · Keri Martinowich[1,3]

Received: 9 February 2018 / Accepted: 21 October 2018 / Published online: 30 October 2018


## Abstract

Signaling of brain-derived neurotrophic factor (BDNF) via tropomyosin receptor kinase B (TrkB) plays a critical role in the maturation of cortical inhibition and controls expression of inhibitory interneuron markers, including the neuropeptide cortistatin (CST). CST is expressed exclusively in a subset of cortical and hippocampal GABAergic interneurons, where it has anticonvulsant effects and controls sleep slow-wave activity (SWA). We hypothesized that CST-expressing interneurons play a critical role in regulating excitatory/inhibitory balance, and that BDNF, signaling through TrkB receptors on CST-expressing interneurons, is required for this function. Ablation of CST-expressing cells caused generalized seizures and premature death during early postnatal development, demonstrating a critical role for these cells in providing inhibition. Mice in which TrkB was selectively deleted from CST-expressing interneurons were hyperactive, slept less and developed spontaneous seizures. Frequencies of spontaneous excitatory post-synaptic currents (sEPSCs) on CST-expressing interneurons were attenuated in these mice. These data suggest that BDNF, signaling through TrkB receptors on CST-expressing cells, promotes excitatory drive onto these cells. Loss of excitatory drive onto CST-expressing cells that lack TrkB receptors may contribute to observed hyperexcitability and epileptogenesis.

**Keywords** BDNF · TrkB · Interneuron · Seizure · Sleep · Cortistatin

## Introduction

Genetic manipulations that decrease activity-dependent brain-derived neurotrophic factor (BDNF) signaling cause down-regulation of transcripts encoding the neuropeptide cortistatin (CST) (Martinowich et al. 2011; Guilloux et al. 2012). CST is a secreted neuropeptide expressed in distinct, although partially overlapping populations of parvalbumin (PV) and somatostatin (SST) expressing inhibitory interneurons in the cerebral cortex and hippocampus (HPC) (de Lecea et al. 1997). CST is structurally similar to SST, but produced from a distinct gene. Indeed, the CST protein was named based on its strong similarity to SST as well as its predominant cortical expression and ability to inhibit cortical activity (de Lecea 2008). While SST and CST can signal via common receptors, they exert distinct biological effects (de Lecea 2008). For example, both peptides increase potassium conductances, but only CST enhances the hyperpolarization-activated cation current ($I_h$) (Schweitzer et al. 2003). In addition, CST infusion prolongs slow-wave sleep duration and increases the magnitude of 0.5–4 Hz sleep slow-wave activity (SWA) (de Lecea et al. 1996; Bourgin et al. 2007). SWA is associated with an increase in BDNF-dependent plasticity during waking, which is diffused with the onset of sleep SWA (Huber et al. 2000, 2007; Tononi 2014). Supporting a link between activity-dependent BDNF signaling and CST-expressing cells, we showed that the sleep-deprivation induced increase in cortistatin (*Cort*) gene expression

**Electronic supplementary material** The online version of this article (https://doi.org/10.1007/s00429-018-1783-1) contains supplementary material, which is available to authorized users.

✉ Keri Martinowich
keri.martinowich@libd.org

[1] Lieber Institute for Brain Development, Johns Hopkins Medical Campus, 855 North Wolfe Street, Suite 300, Baltimore, MD 21205, USA

[2] Sheppard Pratt-Lieber Research Institute, Inc, Baltimore, MD 21204, USA

[3] Departments of Psychiatry and Behavioral Sciences, and Neuroscience, Johns Hopkins University School of Medicine, Baltimore, MD 21205, USA

is blunted in mice with reduced activity-dependent BDNF signaling (Martinowich et al. 2011).

BDNF signals through its cognate receptor tropomyosin receptor kinase B (TrkB) to play a critical role in the maturation of inhibitory interneurons (Marty et al. 1997; Heimel et al. 2011). For example, BDNF-TrkB signaling impacts maturation of PV-expressing interneurons in the visual system following eye opening (Itami et al. 2007; Huang 2013). However, how BDNF-TrkB signaling influences other populations of inhibitory interneurons is not as well understood. CST is expressed in a distinct subset of inhibitory interneurons in the cortex and hippocampus (de Lecea et al. 1997), and appears relatively early in postnatal development compared to other interneuron markers (Taniguchi et al. 2011). In the brain, *Cort* gene expression peaks following the second postnatal week of life in rodents (de Lecea et al. 1997), coinciding with a rapid rise in BDNF levels (Timmusk et al. 1994). Correlations between BDNF signaling and *Cort* expression have been demonstrated in both human and animal studies (Martinowich et al. 2011; Douillard-Guilloux et al. 2012; Ding et al. 2015; Hill et al. 2016; Maynard et al. 2016), suggesting that BDNF-TrkB signaling may impact the development and function of CST-expressing interneurons.

However, whether TrkB signaling in CST-expressing cells directly mediates the impact of BDNF signaling on the function of these cells is not known. To test this hypothesis we deleted TrkB selectively in CST-expressing cells, and found that mutant mice have spontaneous seizures and reduced sleep, as well as reduced excitatory drive onto CST-expressing interneurons. These data suggest that a reduction in the number or density of excitatory connections on CST-expressing cells may contribute to observed hyperexcitability in these mutant animals. Together, the data support a model where BDNF signaling via cell autonomous TrkB signaling in CST-expressing interneurons is critical for their ability to provide adequate inhibitory control.

## Materials and methods

### Animals

We selectively ablated CST-expressing cells by crossing mice driving Cre-recombinase under control of the endogenous *Cort* promoter, (Cort$^{tm1(cre)Zjh}$/J; referenced in text as CST$^{cre}$, stock# 010910, Jackson Laboratory, Bar Harbor, ME) (Taniguchi et al. 2011), to mice carrying a *loxP*-flanked STOP cassette associated with an attenuated diphtheria toxin cassette in the ROSA26 locus (B6; 129-Gt(ROSA)26Sor$^{tm1(DTA)Mrc}$/J; referenced in text as DTA, stock# 010527, Jackson Laboratory). CST$^{cre}$/DTA were used as experimental animals while both CST$^{cre}$ and DTA mice were used as controls. CST$^{cre}$ mice were backcrossed to a C57Bl6/J background > 12X before initiating crosses. Selective TrkB deletion in CST-expressing cells was achieved by crossing CST$^{cre}$ mice to mice harboring a floxed TrkB allele (strain fB/fB, referenced in text as TrkB$^{flox/flox}$) (Grishanin, Yang et al. 2008). TrkB$^{flox/flox}$ mice were backcrossed to a C57Bl6/J background > 5X. CST$^{cre}$/TrkB$^{flox/flox}$ were used as experimental animals and both CST$^{cre}$/TrkB$^{+/+}$ and TrkB$^{flox/flox}$ mice were used as controls. To visualize CST-expressing cells, we crossed CST$^{cre}$/TrkB$^{+/flox}$ mice to mice expressing a *loxP* flanked STOP cassette in the *Gt(ROSA)26Sor* locus, which prevents transcription of the tdTomato reporter in the absence of Cre-mediated recombination (B6.Cg-Gt(ROSA)26Sor$^{tm14(CAG-tdTomato)Hze}$/J; referenced in text as tdTOM, stock# 007909, Jackson Laboratory). In these experiments CST$^{cre}$/TrkB$^{flox/flox}$/tdTOM mutant mice were compared to CST$^{cre}$/TrkB$^{+/+}$/tdTOM mice as controls.

Mice were group-housed (3–5 animals per cage) in standard caging (Innovive, San Diego, CA) unless otherwise described. Cages were housed in a temperature and humidity controlled environment with a 12:12 light/dark cycle and animals had ad libitum access to standard rodent chow and water. Procedures for animal care and use were approved by the Institutional Animal Care and Use Committee (SoBran Biosciences, Baltimore, MD). Male and female mice were included and analyzed in all experiments.

### Developmental behavioral analysis

Observations of tremors, seizure severity, hindlimb clasping, and survival were recorded daily. For tremor observation, mouse pups were placed in compartments of a plastic box for 30 min and spontaneous movement was scored (Price et al. 2009). Presence of seizures was determined during homecage observations made three times a day for 1 h, 3 h apart, and scored for severity using a modified Racine scale (Luttjohann et al. 2009). A pre-determined scoring system was used to characterize each animal's overall seizure behavior. Individual seizure behaviors (including observations of behavioral arrest, unilateral or bilateral clasping, head bobbing, forelimb clonus, rearing and falling) were noted. Hindlimb clasping was measured by picking up each animal by its tail and suspending it 150 mm above a surface for 2 min. Total duration of both hindlimb and forelimb clasping were independently measured. Mice were scored on a "yes" or "no" basis, with a clasping event being defined as retraction of one or both hindlimbs toward the midline (Baquet et al. 2004).

### RNA extraction and quantitative RT-PCR (qPCR)

Mice were euthanized by cervical dislocation and dissected tissue was snap frozen in isopentane and stored at − 80 °C. qPCR was performed as described previously (Maynard et al. 2016). Briefly, total RNA was isolated and extracted using TRIzol (Life Technologies, Carlsbad, CA). RNA was then purified using RNeasy minicolumns (Qiagen, Valencia, CA) and quantified by a NanoDrop spectrophotometer (Agilent Technologies, Savage, MD). RNA concentration was normalized and reverse transcribed into single-stranded cDNA using Superscript III (Life Technologies). Quantitative PCR was performed using a Realplex Thermocycler (Eppendorf, Hamburg, Germany) using GEMM Mastermix (Life Technologies) with 40 ng of synthesized cDNA. Individual mRNA levels were normalized for each well to *Gapdh* mRNA levels.

### Immunohistochemistry

Mice were anesthetized and transcardially perfused with 4% paraformaldehyde. Brains were post-fixed overnight, cryoprotected in 30% sucrose, and serial sections were cut using a microtome (Leica Biosystems Inc., Wetzlar, Germany) equipped with a freezing stage (Physitemp, Cliffton, NJ). For fluorescence co-labeling experiments, free-floating sections were incubated with anti-TrkB, anti-PV, biotin-conjugated lectin from *Wisteria floribunda* (WFA), anti-SST and anti-Glutamate decarboxylase (GAD67). Sections were washed 3X in phosphate buffered saline (PBS), incubated in 50 mM ammonium chloride in PBS for 1 h at room temperature, and blocked in 10% normal goat serum (NGS) with 0.1% Triton-X 100 for 30 min at 25 °C. Sections were washed and incubated in anti-TrkB H-181 (1:300, sc-8316, Santa Cruz Biotechnology, Santa Cruz, CA), WFA (1:200, L1516, Sigma–Aldrich, St. Louis, MO), anti-PV (1:1000, P3088, Sigma–Aldrich) and anti-SST (1:400, MAB354, EMD Millipore, Darmstadt, Germany) at 4 °C overnight in 2% NGS. For GAD67 staining, sections were washed and blocked in 0.3% DMSO rather than Triton X and incubated for 4 days with anti-GAD67 (1:500, MAB5406, Millipore, Temecula, CA) at 4 °C in 2% NGS. After primary incubation, sections were conjugated with secondary antibodies, either an Alexa Fluor 555 (1:250, A21422, ThermoFisher, Halethorpe, MD) or a streptavidin Alexa Fluor 488 (1:400, S32354, ThermoFisher). Sections were rinsed in PBS for 10 min, placed in 0.1% Sudan Black for 2 h to block auto-fluorescence, counterstained with DAPI (1:10,000, Thermo Fisher) for 5 min, rinsed for 30 min and mounted with Immu-mount (ThermoFisher), for imaging. For anti-RFP Diaminobenzidine (DAB) staining, sections were washed in 0.1% Tween 20 in PBS for 30 min, blocked with 3% NGS in 0.1% Tween 20 for 30 min at 25 °C, then washed and incubated in anti-RFP (1:500, ab34771, Abcam, Cambridge, MA) at 4 °C overnight in 2% NGS. After incubation, sections were washed for 10 min in PBS after which the VectorStain Kit ABC horseradish peroxidase prep (HRP) application was used per the manufacturers instructions (Vector Laboratories, Inc., Burlingame, CA). Sections were incubated in ABC-HRP for 1 h and then rinsed for 20 min in PBS. To block endogenous peroxidase activity, 0.3% peroxide in water was added to sections after rinsing for 30 min. Finally, sections were stained for 3 min using Sigmafast cobalt DAB metal enhancer tablets (Sigma–Aldrich), rinsed in PBS, mounted, counterstained with Nissl, coverslipped with Permount (ThermoFisher) and imaged. Three sections per animal were counted and analyzed by a blinded rater.

### Automated homecage behavior monitoring

Homecage monitoring was conducted similarly to previous descriptions (Martinowich et al. 2011, 2012). Briefly, a single animal was placed into a standard housing cage that contained food, bedding and water. This cage was then placed within a temperature and humidity controlled automated home cage recording chamber system for 48 h. The chamber contained white lights for light-phase illumination and infrared lights for dark phase recording, and was programmed to be in sync with the animal's normal 12:12 lights on/lights off cycle in the holding facility. The first 24 h were considered an acclimation period and not analyzed. The second 24 h were used for data analysis. Behavior was automatically analyzed in real-time using HomeCageScan software (CleverSys Inc, Reston, VA). Animal positioning and sequence of movements were used to analyze patterns of complex behavior in durations > 6 frames (30 frames/s).

### Headstage implantation surgery and in vivo electrophysiology recording with simultaneous video monitoring

P21 aged mice received inhaled isoflurane anesthesia during the surgery to implant custom-built recording headstages. Electronic hardware boards (Electronic Hardware LTD, Hollywood, CA) cut into 8-pin segments were used as the headstage base. Silver wires (0.33 mm, A-M Systems, Carlsborg, WA) soldered to gold pins were inserted into the headstage and used as surface recording electrodes. A custom-made bipolar twisted wire depth electrode attached to a pin (Pinnacle Technologies, Lawrence, KS) was also inserted into the headstage. To compensate for developmental differences in targeting, stereotaxic locations were calculated using the bregma-lambda scaling technique (Moore and Boehm 2009). A scaling ratio was created by obtaining the bregma-lambda distance for the mouse and then dividing by 4.21, which is the average value for adult C57BL/6J mice. This ratio

number was then multiplied by each of the desired adult coordinates. The following reported coordinates are thus based on the desired adult Paxinos-Franklin coordinates. The reference electrode was placed in the right frontal cortex + 2 Anterior-Posterior (AP), 1.5 Medial–Lateral (ML) and the ground electrode was placed near bregma (− 1 AP, + 1.5 ML). An additional electrode was placed over the parietal cortex (− 2.4 AP, − 3 ML), and the depth electrode was targeted to the CA1 region in the opposite hemisphere in the hippocampus − 2.4 AP, + 3 ML, − 1.62 dorsal–ventral (DV). The headmount was fixed to the skull using dental acrylic (OrthoJet, Lang Dental, Wheeling, IL). Mice were administered 1.5 mg/kg meloxicam intraperitoneal for 3d post-surgery.

Following headstage implant, mice were serially recorded starting at P26, continuing on P30, P32, P34, P37, and P41 or until death. Each day, mice were placed in the homecage recording set-up described above, and video and electrophysiological recordings were simultaneously made during the light cycle for 3.5 h. Electroencephalogram (EEG) from surface electrodes and HPC local field potential (LFP) data from the HPC depth electrode was recorded using Sirenia Acquisition hardware and software (Pinnacle Technologies, Lawrence KS) at a rate of 2000 Hz. Video was captured using CaptureStar software (CleverSys Inc). Successful placement of the HPC depth electrode was confirmed post-mortem using Nissl staining following perfusion (Fig. S4A).

## In vivo electrophysiology data analysis

Custom Matlab (Mathworks, Natick, MA) scripts were created for the analysis of electrophysiological data. Raw .edf files for each session were converted to .mat files for further analysis. The Matlab pwelch function, which uses Welch's overlapped segment averaging estimator, was used to calculate power spectral density (PSD). The data window was 4000 samples (2 s), the amount of data overlap used was 50%, and the number of discrete Fourier transform points used in the calculation was 4096. This number of transform points was chosen because it is the next higher power of 2 above 4000, allowing for faster computation time. The spectrum was decibel (dB)-scaled prior to plotting, and the reported results reflect absolute values. For feature detection of seizures, we also performed line length analysis (Estellar 2001): Session data were segmented into 2 s epochs and within each epoch, the sum of the distance between successive data points was calculated, and then converted to an absolute value. The line length for each epoch was estimated by summing the absolute value of the distance between all points, and then the mean line length value for the session was determined. Seizures were identified by finding epochs with line length values two standard deviations above the mean value. For PSD analysis of line length data, either 2 s potential seizure or non-seizure epochs were combined into a continuous data file for each animal and then pwelch analysis was performed on both sets of epochs as described.

## In vitro electrophysiological recordings of CST interneuron excitability

3–4 week old control (Ctrl, $CST^{cre}/TrkB^{+/+}$/tdTOM) and mutant mice ($CST^{cre}/TrkB^{flox/flox}$/tdTOM) were sacrificed following isoflurane administration. The brains were quickly removed, and 300-µm thick coronal slices containing somatosensory cortex were cut on a Leica VT1000 S Vibrating blade microtome (Leica Biosystems Inc.). The slices were maintained in oxygenated ice-cold $Na^+$-free sucrose solution containing 2.5 mM KCl, 1.25 mM $NaH_2PO_4$, 26 mM $NaHCO_3$, 0.5 mM $CaCl_2$, 4.0 mM $MgCl_2$, and 250 mM sucrose. The slices were initially incubated at 34 °C in a Ringer solution (ACSF) containing 125 mM NaCl, 2.5 mM KCl, 1.25 mM $NaH_2PO_4$, 2 mM $CaCl_2$, 1 mM $MgCl_2$, 26 mM $NaHCO_3$ and 10 mM dextrose, pH 7.4, and then kept at room temperature. Slices were equilibrated for at least 30 min before recording. The slices were transferred into a recording chamber at approximately 32–34 °C. For current clamp, the recording pipettes were filled with intracellular solution containing (in mM) 130 K-gluconate, 1 $MgCl_2$, 5 EGTA, 5 MgATP, 10 HEPES and 0.4 $Na_2GTP$ (pH 7.2 with KOH). The resistances of patch pipettes were 4–7 MΩ. The signals were amplified and filtered at 2 kHz with Axopatch 200B (Molecular Devices, Sunnyvale, CA) and acquired at sampling intervals of 20–100 µs through a DigiData 1321A interface with program pCLAMP 10 (Molecular Devices, Sunnyvale, CA). The access resistance was monitored during recordings, and the data were excluded from analysis if the series resistance changed more than 20% from control levels (10–25 MΩ). The frequency (event number) and amplitude of individual events were examined with Clampfit 10 (Molecular Devices). The input resistances of the tested neurons were calculated offline from the voltage produced by negative current injection (− 20 pA) prior to the step currents.

## Statistical methods

Statistics were calculated using GraphPad Prism Software (GraphPad Software, La Jolla, CA). For all animal studies (behavior, electrophysiology and immunohistochemistry), the reported *N* represent independent biological replicates. These *N* are reported in both the Methods section as well as in the individual figure legends for the respective experiments. Group sizes for all studies were based on previous investigations carrying out similar experimental studies (Klaassen et al. 2006; Rossignol et al. 2013; Maynard et al. 2016). Data comparing single averaged values between two

genotypes was compared using an unpaired Student's *t*-test, including qPCR data, homecage behavioral data comparisons, between-genotype power analysis, and cell counting. A paired Student's *t*-test was used for within-genotype comparisons for data from the same mice across conditions, such as spectral power between seizure and non-seizure epochs of CST$^{cre}$/TrkB$^{flox/flox}$ mice. For data comparing changes in *Cort* expression in mice across development, a one-way repeated measures (RM) ANOVA was used. To analyze genotype differences across multiple conditions or time points, such as hindlimb clasping, a two-way RM ANOVA was utilized. For survival data, groups were compared using survival curve comparison. A log-rank (Mantel-Cox) test was performed on data across lifespan.

## Results

### Loss of CST-expressing interneurons causes spontaneous seizures

Mice with reduced activity-dependent BDNF signaling (BDNF-KIV mice) exhibit ~ 2.5 fold down-regulation in expression of *Cort* mRNA transcripts (Martinowich et al. 2011). They also exhibit more severe seizures, higher mortality and increased seizure susceptibility compared to WT animals (Fig. S1A-C). To determine whether CST-expressing interneurons influence seizure progression and severity, we investigated the effect of ablating this cell population by crossing CST$^{cre}$ mice to mice carrying a *loxP*-flanked STOP cassette associated with an attenuated diptheria toxin cassette (CST$^{cre}$/DTA mice, Fig. 1a). CST$^{cre}$/DTA mice develop tremors and spasms beginning at P11, which become increasingly common by P17 (Fig. 1b). CST$^{cre}$/DTA mice exhibit premature death starting at P18 with all mutant mice dying by P23 following severe seizure activity (Fig. 1c). Consistent with excessive levels of excitation, CST$^{cre}$/DTA mice showed increased cortical levels of the immediate early genes, *Fos* and *Arc* (Fig. 1d).

### Developmental expression of CST-expressing interneurons

To better understand how CST-expressing interneurons contribute to seizure onset and progression, we characterized development of this cell population. Consistent with previous reports (de Lecea et al. 1997), expression of *Cort* mRNA transcripts peaks during the second week of postnatal life

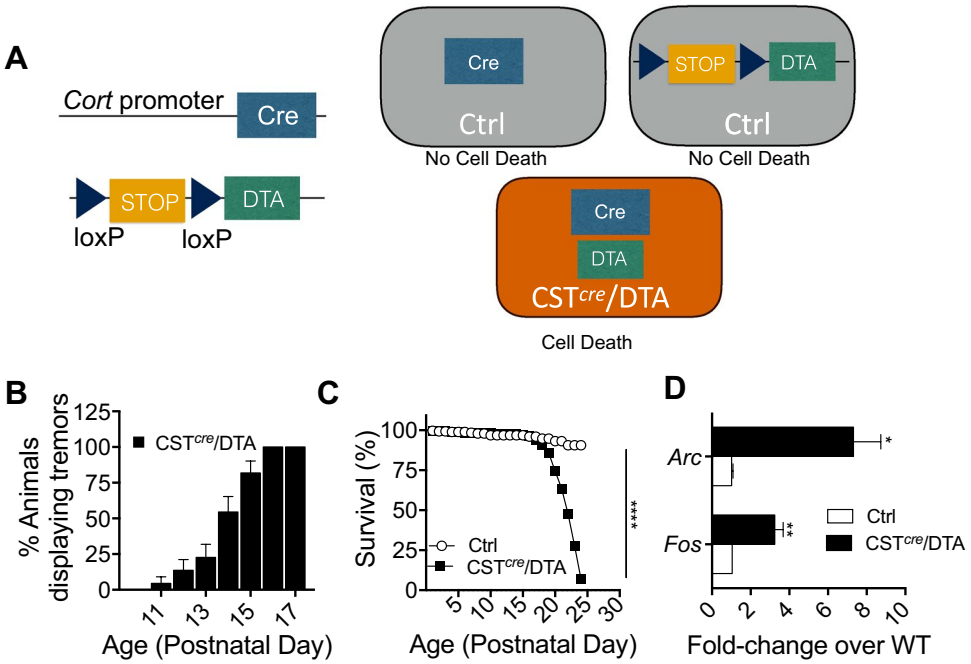


**Fig. 1** Selective ablation of Cortistatin (CST)-interneurons causes increased excitation, seizures and death. **a** Schematic describing deletion strategy. CST$^{cre}$ mice were crossed to mice with a *loxP*-flanked STOP cassette associated with an attenuated diphtheria toxin cassette (DTA). Expression of Cre-recombinase in CST-positive cells causes expression of diphtheria toxin and selective cell ablation. **b** CST$^{cre}$/DTA mice develop tremors beginning on P11 ($n=22$). **c** CST$^{cre}$/DTA mice die between P18 and P23, significantly earlier than Control (Ctrl) mice ($n=22$/genotype, Mantel-Cox log-rank test, $p<0.0001$). **d** Immediate early gene transcripts are increased in the cortex of CST$^{cre}$/DTA mice. Quantitative PCR (qPCR) shows a 3.2 fold increase in *Fos* (*t*-test, $p=0.0087$) and a 7.3 fold increase in *Arc* (*t*-test, $p=0.0112$) ($n=3$/group). Data are represented as mean ± standard error of the mean (SEM) (*$p<0.05$, **$p<0.01$, ****$p<0.0001$)

expression in WT animals (Fig. 2a). To identify CST-expressing cells, we crossed CST$^{cre}$ mice with Rosa26-Lox-STOP-Lox tdTomato reporter mice (tdTOM), resulting in red fluorescent labeling only in CST$^{cre}$-expressing interneurons. Figure 2b demonstrates cortical expression of CST-positive tdTOM labeled cells during early postnatal development. Consistent with a previous report (de Lecea et al. 1997), nearly all CST interneurons express GAD67 and their cell bodies are more densely localized in layers 5/6 compared to layers 2/3, but nearly absent from layer 4 (Fig. 2b–d). We quantified labeling with other interneuron markers (Fig. 2d) and found significant overlap of CST-expressing cells with SST (44.7 ± 4.3%) and calbindin (CB) (24.3 ± 4.7%), and association of 33 ± 1.7% of CST-expressing cells with a perineuronal net (PNN). Consistent with a previous report describing this CST$^{cre}$ mouse line (Taniguchi et al. 2011), there is less overlap of CST-expressing interneurons with PV (15.33 ± 4.3%). CST-expressing cells are almost never

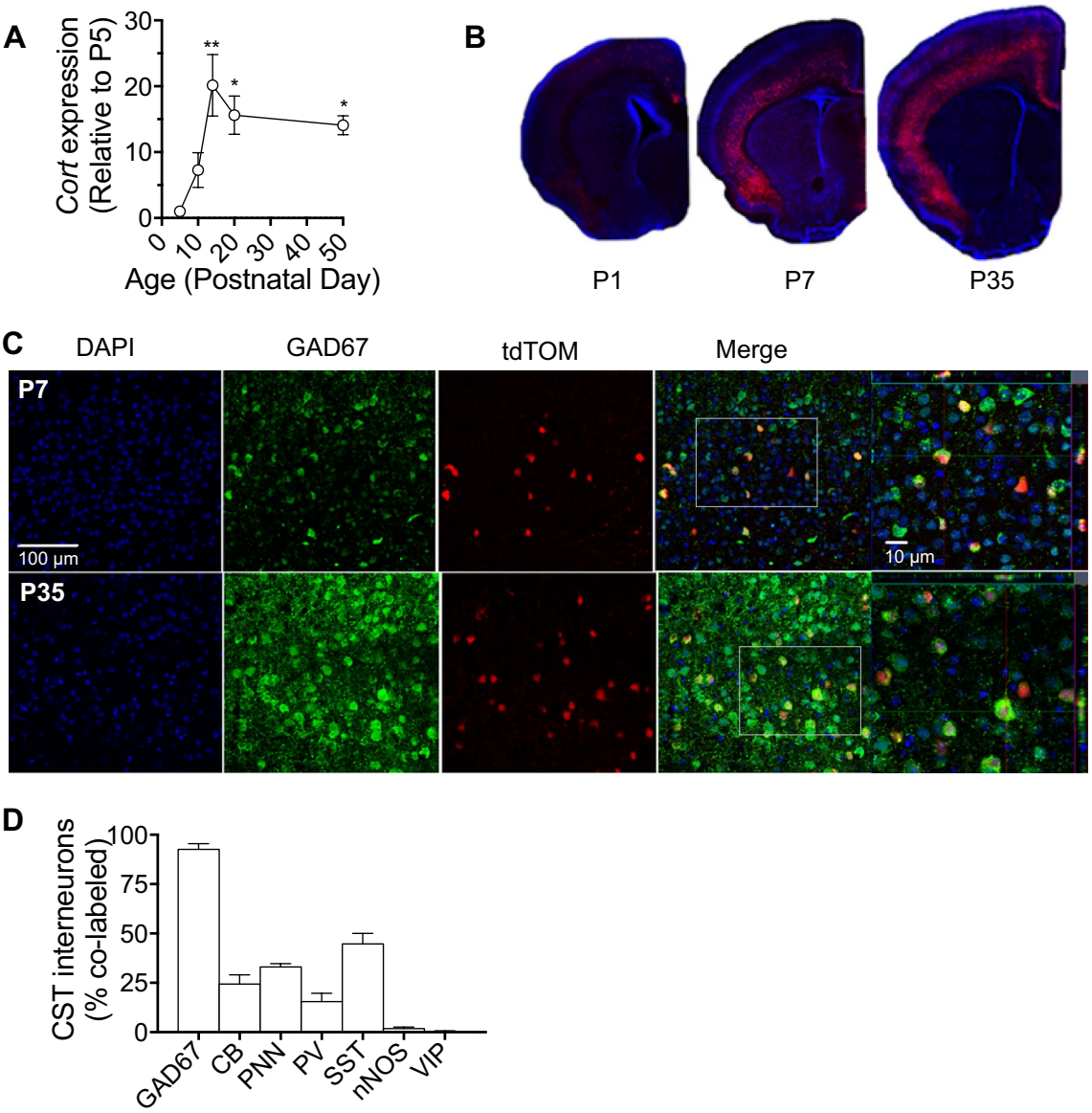


**Fig. 2** Developmental expression of *Cort* and co-expression of CST interneurons with interneuron markers. **a** qPCR demonstrates the time course of cortical *Cort* expression across development, which peaks in the second and third postnatal weeks (1-way ANOVA, $p = 0.0055$, post-hoc *t*-tests, P5:P14-$p < 0.001$, P5:P20 and P5:P50, $p < 0.05$). Data are represented as fold changed relative to P5. **b** Representative images depicting cortical expression of tdTomato (tdTOM) labeled CST-interneurons across early postnatal development. **c** Representative images demonstrating co-labeling of tdTOM labeled CST interneurons and inhibitory enzyme Glutamate decarboxylase 67 (GAD67) at P7 and P35. **d** Percent co-labeling of tdTOM labeled CST interneurons in somatosensory cortex (S1) of 6 week old mice ($n = 3$). Data are represented as mean ± SEM (*$p < 0.05$, **$p < 0.01$)

positive for nitric oxide synthase (nNOS) (1.7 ± 0.9%) or vasoactive-intestinal peptide (VIP) (0.3 ± 0.3%).

## Selective TrkB deletion in CST-expressing cells causes spontaneous seizures

We next asked whether BDNF/TrkB signaling is required for CST-expressing interneurons to control E/I balance. To selectively delete TrkB in CST-expressing interneurons, we crossed mice harboring a floxed TrkB allele (TrkB$^{flox/flox}$) with CST$^{cre}$ mice (Fig. S2A). We conducted a developmental behavioral study in CST$^{cre}$/TrkB$^{flox/flox}$ mice and observed abnormal hindlimb clasping by P15 (Fig. 3a, b). Automated homecage behavior testing at P21 revealed hyperactivity, reduced sleep, and repetitive jumping in CST$^{cre}$/TrkB$^{flox/flox}$ mice (Fig. 3c–d). Spontaneous seizures were detected in CST$^{cre}$/TrkB$^{flox/flox}$ mice by P21 (Fig. 3f), and most CST$^{cre}$/TrkB$^{flox/flox}$ mice died between 5 and 6 weeks of age (Fig. 3g). In a subset of mice, we inter-crossed CST$^{cre}$/TrkB$^{flox/flox}$ mice to tdTOM mice to label CST-expressing interneurons (Fig. S2A). Immunohistochemical studies in CST$^{cre}$/TrkB$^{flox/flox}$ mice confirmed TrkB loss in CST-expressing interneurons

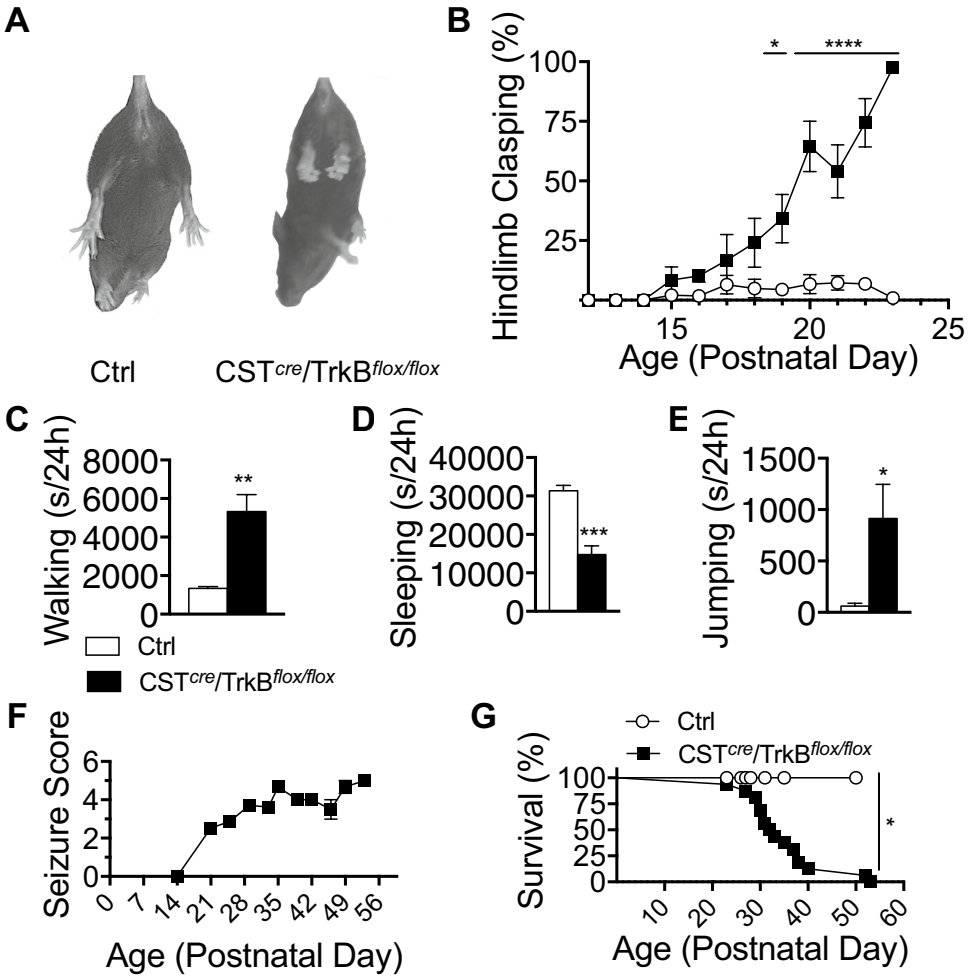


**Fig. 3** Selective deletion of Tropomyosin Receptor Kinase B (TrkB) in CST-expressing cells results in motor impairments, hyperactivity, seizures and death. **a** Representative photo of hindlimb clasping in CST$^{cre}$/TrkB$^{flox/flox}$ mice, in which limbs retract inwards towards the midline. **b** CST$^{cre}$/TrkB$^{flox/flox}$ mice develop hindlimb clasping behavior, which is not observed in Ctrl mice ($n=6$ Ctrl, $n=7$ CST$^{cre}$/TrkB$^{flox/flox}$; 2-way RM ANOVA, genotype effect, $p<0.0001$ and genotype-time interaction, $p<0.001$. Post-hoc tests revealed genotype-dependent differences from P19 to P23, P19-$p<0.05$, P20-23- $p<0.0001$). CST$^{cre}$/TrkB$^{flox/flox}$ mice exhibit hyperactivity in the homecage. Data are displayed as total seconds engaging in the behavior in a 24 h period ($n=4$/group). **c** CST$^{cre}$/TrkB$^{flox/flox}$ mice spend more time walking than Ctrl mice ($t$-test, $p=0.0038$). **d** CST$^{cre}$/TrkB$^{flox/flox}$ mice sleep less than Ctrl mice ($t$ test, $p=0.0008$). **e** Increased repetitive jumping activity in CST$^{cre}$/TrkB$^{flox/flox}$ mice ($t$-test, $p=0.0428$). **f** Racine scores of seizures observed in CST$^{cre}$/TrkB$^{flox/flox}$. Seizure onset occurred at P21, and progressed in severity until death. No seizures were observed in Ctrl mice ($n=19$/group). **g** Survival data for CST$^{cre}$/TrkB$^{flox/flox}$. 50% of mutants die by P32, and the majority die by 5–6 weeks postnatal ($n=15$ Ctrl, $n=8$ CST$^{cre}$/TrkB$^{flox/flox}$) (Mantel-Cox log-rank test, $p=0.0173$). Data are represented as mean ± SEM (*$p<0.05$, **$p<0.01$, ***$p<0.001$, **** $p<0.0001$)

(Fig. S2B-C). To determine whether the observed seizure phenotype is specific to TrkB deletion from CST- expressing interneurons, we examined the effect of deleting TrkB in PV-expressing interneurons. We crossed PV$^{cre}$ mice with TrkB$^{flox/flox}$ mice to delete TrkB specifically in PV-expressing cells. Consistent with previous reports (Lucas et al. 2014), we found that PV$^{cre}$/TrkB$^{flox/flox}$ mice exhibit motor impairments, including stereotyped circling behavior in the open field, decreased latency to fall on an accelerating rotorod, and impaired grip strength (Fig. S3A-C). However, these animals do not develop spontaneous seizures and live to at least 5 months of age (data not shown).

## Characterization of seizures in CST/TrkB$^{flox/flox}$ mice

To understand how loss of TrkB in CST-expressing cells contributes to development of spontaneous seizures, we monitored seizure progression using video-EEG in CST$^{cre}$/TrkB$^{flox/flox}$ mice. Mice were surgically implanted with headstages at P21 that contained cortical surface electrodes for EEG and an HPC depth electrode targeted to CA1 to record local field potentials (LFP) (Fig. 4a, S4A). We consistently observed an increase in the amplitude of EEG activity in CST$^{cre}$/TrkB$^{flox/flox}$ mice compared to Ctrl (Fig. 4c–e). Because 5/6 CST$^{cre}$/TrkB$^{flox/flox}$ mice died on or prior to P34, quantitative analysis was conducted on data recorded from P26-P32. CST$^{cre}$/TrkB$^{flox/flox}$ mice displayed seizures of varying intensity within a session, which were accompanied by abnormal EEG patterns (Fig. 4b). Common seizure types observed included absence (behavioral arrest with automatisms and myoclonus), clonic, and generalized tonic-clonic (Supplementary Videos). Using power spectral density estimation on EEG data collected at P26 prior to any seizure-induced deaths, CST$^{cre}$/TrkB$^{flox/flox}$ mice exhibit increased 25–40 Hz power across the session (Fig. 4c, d). We noted that seizures in CST$^{cre}$/TrkB$^{flox/flox}$ mice typically begin in the cortex and migrate to HPC with increasing severity (Fig. S4). 5/6 CST$^{cre}$/TrkB$^{flox/flox}$ mice had analyzable LFP signals from the CA1 electrode, and 3 of those 5 exhibited an increase in high amplitude sharp-wave discharge (SWD)

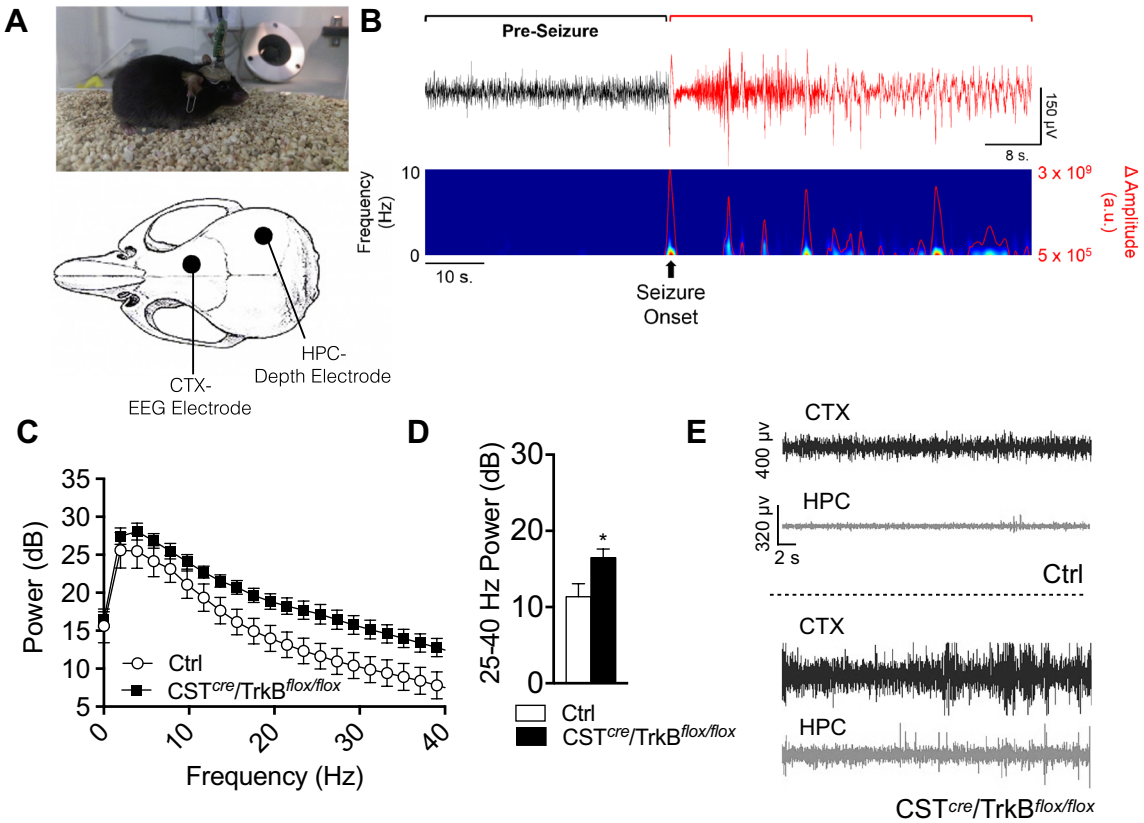


**Fig. 4** Mice with selective TrkB deletion in CST-expressing interneurons exhibit abnormal electroencephalogram (EEG) activity. **a** Video-EEG set up (upper) and placement of cortical (CTX) EEG electrode and hippocampal (HPC) depth electrode (lower). **b** Example HPC local field potential (LFP) trace (top panel) and corresponding heat map (bottom panel) recorded from a CST$^{cre}$/TrkB$^{flox/flox}$ mouse at P32 during seizure. **c** Power spectral density (PSD) comparison for Ctrl and CST$^{cre}$/TrkB$^{flox/flox}$ mice, from P26 total session data. ($n=6$/group). **d** P26 average 25–40 Hz power estimates demonstrate that CST$^{cre}$/TrkB$^{flox/flox}$ mice exhibit an increase in high frequency power ($t$-test, $p=0.0339$). **f** 30 s representative examples of EEG and HPC signal at P32, from Ctrl (upper) and CST$^{cre}$/TrkB$^{flox/flox}$ mice (lower)

with increased seizure severity (Fig.S4). Spectrogram data of SWD events indicated a broadband increase in power (Fig.S4E), and in the final recording at P32, there was an increase in HPC SWDs (Fig. S4F-G).

### Effects of TrkB loss in CST-expressing cells on their migration, survival and physiology

Because TrkB can mediate neurotrophic effects of BDNF, we examined whether loss of TrkB in CST-expressing interneurons caused abnormal migration, organization, or death of these cells. We quantified the numbers of CST-expressing interneurons in CST$^{cre}$/TrkB$^{+/+}$/tdTOM (Ctrl) and CST$^{cre}$/TrkB$^{flox/flox}$/tdTOM mice in the dentate gyrus (DG) and hippocampal CA1/CA3, as well as in superficial and deep layers of somatosensory cortex (S1) (Fig. S5A-D). In HPC, there was no difference in the number of CST-expressing interneurons in DG or CA1/CA3 regions (Fig. S5B), and in S1 there was no difference in the total number of CST-expressing interneurons (Fig. S5C). Cell counts in layers 2/3 and in layers 5/6 of S1 revealed similar numbers of CST-expressing cells between Ctrl and CST$^{cre}$/TrkB$^{flox/flox}$/tdTOM animals (Fig. S5D). We next used fluorescent immunostaining to determine whether survival of any specific sub-population of CST-expressing interneurons was affected by TrkB deletion. The data revealed no difference in total number of cells co-expressing PV or SST, or surrounded by a PNN between genotypes (Fig. S5E). Together, the results suggest that TrkB deletion in CST-expressing cells does not cause gross deficits in their migration, localization or survival.

To better assess the physiological consequences of TrkB loss in CST-expressing interneurons that could cause the observed behavioral impairments and development of seizures in CST$^{cre}$/TrkB$^{flox/flox}$ animals, we examined whether GABA release from CST-expressing cells was impaired. Because CST-expressing cells are sparse, assessing inhibitory transmission events using paired-recordings is difficult due to low connection probability. Hence, we took an alternative optogenetic approach to assess GABA release properties from CST-expressing cells. We stereotaxically infused a *Cre*-dependent AAV9 channelrhodopsin (ChR2):tdTOM viral vector in Ctrl and CST$^{cre}$/TrkB$^{flox/flox}$ mice, resulting in ChR2 expression exclusively in CST interneurons (Fig. S7). We then stimulated GABA release in these cells by fiber-optic light activation of ChR2 in ex-vivo cortical slices from Ctrl and CST$^{cre}$/TrkB$^{flox/flox}$ mice (Fig. S7). Comparison of genotypes revealed no significant differences in inhibitory post-synaptic currents (IPSCs) between pulses, recorded as percent depression (Fig. S7), suggesting that synaptic transmission from CST-expressing cells is not affected by TrkB deletion.

We next assessed whether TrkB influences electrophysiological maturation of CST-expressing cells by measuring excitability of layer 2/3 CST-positive interneurons in Ctrl and CST$^{cre}$/TrkB$^{flox/flox}$/tdTOM mice. We found no difference in intrinsic excitability as demonstrated by similar numbers of action potentials fired in response to depolarizing current steps (Fig. S6A-B), and no difference was observed in the baseline membrane properties of CST-expressing cells in CST$^{cre}$/TrkB$^{flox/flox}$/tdTOM mice (Fig. S6C). Alterations in excitatory drive to interneurons provide another potential mechanism that could explain observed impairments in inhibition and altered E/I balance. Hence, we asked whether loss of TrkB in CST-expressing interneurons affects glutamate-mediated excitation of CST-expressing interneurons in CST$^{cre}$/TrkB$^{flox/flox}$/tdTOM mice. We made successful whole cell recordings in visually identified tdTOM + interneurons in S1 of cortical slices and recorded spontaneous ePSCs. These experiments showed no change in amplitude, rise time or decay time (Fig. 5c–h), but did reveal significantly decreased sEPSC frequencies (Fig. 5b).

## Discussion

BDNF-TrkB signaling is implicated in the etiology of epilepsy. In particular, its role in the transformation of the brain during chronic temporal lobe epilepsy (TLE) has been extensively studied (Reibel et al. 2001; Koyama and Ikegaya 2005; McNamara and Scharfman 2012). Because BDNF is a potent regulator of activity-dependent synaptic plasticity and plays key roles in the developing GABAergic circuitry, it exerts significant control over E/I balance (Nagappan and Lu 2005; Woo and Lu 2006). However, there are conflicting reports about when and where BDNF-TrkB signaling facilitates excitation versus inhibition to promote or attenuate seizures and epilepsy (Koyama and Ikegaya 2005). Specifically, several lines of evidence demonstrated that BDNF-TrkB signaling is increased following neuronal insults or kindling, and that antagonizing its signaling can slow seizure onset and decrease seizure severity (Ernfors et al. 1991; Merlio et al. 1993; Binder et al. 1999; Liu et al. 2014). Alternatively, other studies show that BDNF infusion can promote inhibitory signaling and delay seizure onset (Reibel et al. 2001; Paradiso et al. 2011; Simonato 2014; Prince et al. 2016). While the role of BDNF-TrkB signaling in models of induced epilepsy in adults is well-studied, its role in the onset of idiopathic, spontaneous epilepsy during development is less clear (Weidner et al. 2014). Since TrkB antagonism is proposed as a therapeutic treatment for epilepsy (McNamara and Scharfman 2012; Liu et al. 2014), a complete understanding of how BDNF-TrkB signaling modulates brain excitability is important. Our study is notable because the role played by differential effects of cell-autonomous TrkB signaling in inhibitory interneurons versus excitatory cells in the context of epilepsy has not yet

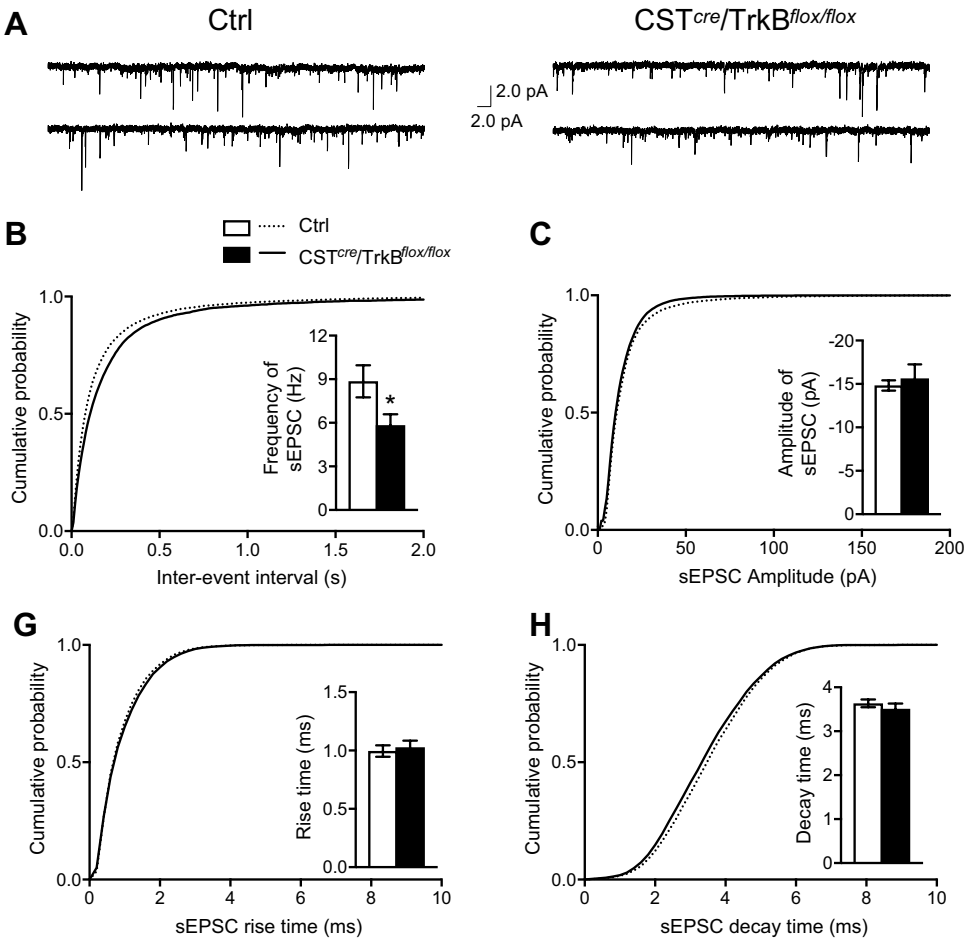


**Fig. 5** Glutamatergic basal transmission onto CST interneurons in CST$^{cre}$/TrkB$^{flox/flox}$ mice. **a** Sample traces of spontaneous excitatory postsynaptic currents (sEPSCs) recorded from the layer 2/3 CST interneurons of S1 cortex in control (Ctrl) mice (left panel) and CST$^{cre}$/TrkB$^{flox/flox}$ mice (right panel). Cumulative plots and histograms of sEPSC frequency (inter-event intervals) ($p < 0.05$) (**b**), amplitude (**c**), rise time (**d**) and decay time (**e**) recorded from the layer 2/3 CST interneurons in Ctrl and CST$^{cre}$/TrkB$^{flox/flox}$ mice. Data were analyzed by student *t* test and Kolmogorov–Smirnov test

been explored. BDNF is primarily synthesized and secreted from pyramidal cells, but is absent from inhibitory interneurons (Cellerino et al. 1996; Gorba and Wahle 1999; Swanwick et al. 2004). While TrkB is expressed on both excitatory and inhibitory neurons, the respective contributions of its signaling in one versus the other in seizure development and epilepsy is not clearly established. While it is known that activity-dependent BDNF signaling controls PV interneuron maturation during ocular dominance development (Huang et al. 1999; Itami et al. 2007; Heimel et al. 2011), the role of BDNF-TrkB signaling in the development of other inhibitory interneuron populations is less well-explored.

Despite constituting a relatively sparse subpopulation of interneurons whose localization is restricted to the HPC and cortex, CST-expressing interneurons are required for E/I balance, as demonstrated by our data showing that their ablation causes spontaneous seizures and premature death. CST signaling is implicated in both neuroprotection and regulation of sleep homeostasis. Intraventricular and intrahippocampal CST infusion attenuates severity of chemoconvulsant-induced seizures and prevents hippocampal cell death (Braun et al. 1998; Aourz et al. 2014). In addition to attenuating seizures, both CST and BDNF-TrkB signaling directly impact sleep physiology. Brain infusion of BDNF and CST increases the magnitude of low-frequency SWA during slow-wave sleep (de Lecea et al. 1996; Bourgin et al. 2007; Faraguna et al. 2008), the onset of which coincides with developmental upregulation of *Bdnf* and *Cort* expression (Hairston et al. 2011). We previously showed reduced *Cort* expression and SWA in mice with decreased activity-dependent BDNF (Hill et al. 2016), and here we demonstrate that animals in which TrkB is selectively deleted in CST-expressing cells sleep significantly less than controls. These findings support a mechanistic link between BDNF, *Cort* expression and sleep physiology. CST may increase SWA by augmenting the hyperpolarizing $I_h$ current, resulting in increased synchronous oscillation in the cortex and HPC (Schweitzer et al. 2003; de Lecea 2008). This is intriguing because mutations in the gene encoding HCN1, the channel which regulates $I_h$, cause infantile epilepsy (Poolos 2012; Nava et al. 2014), and TrkB and HCN1 are co-expressed in cells controlling synchronized oscillatory activity (Thoby-Brisson et al. 2003).

Beyond epilepsy, the interaction between CST and BDNF-TrkB signaling may have implications for neurodevelopmental disorders and major depressive disorder

(MDD). Interestingly, genes that are misregulated in the brains of individuals with autism spectrum disorder (ASD) and candidate genes discovered in clinical studies of ASD are over-represented in the translatome of CST-expressing cells (Xu et al. 2014; Chang et al. 2015). In addition to sleep impairments, $CST^{cre}/TrkB^{flox/flox}$ mice exhibit repetitive jumping behavior, consistent with a number of mouse models of neurodevelopmental disorders (Patterson 2011). Furthermore, co-morbidity between ASD and seizure disorders is high, suggesting a possible mechanistic link in the underlying biology (Jacob 2016). Decreased expression of *BDNF, CORT* and *SST* are noted in animal models of depression and in postmortem human studies of adults with MDD (Guilloux et al. 2012; Ding et al. 2015; Lin and Sibille 2015). SST knockout mice show increased anxiety/depressive-like behaviors as well as downregulation of *Bdnf* and *Cort* (Lin and Sibille 2015), and mice with a deletion of the *Cort* gene exhibit increased anxiety (Souza-Moreira et al. 2013). Functional studies recently showed that disinhibiting forebrain SST-expressing interneurons causes anti-depressive and anti-anxiolytic effects (Fuchs et al. 2017). Thus, understanding the mechanisms underlying BDNF-TrkB signaling in CST-expressing interneurons could generate new insights into MDD treatment.

In summary, we discovered an essential role for CST-expressing interneurons in controlling E/I balance, a function that requires intact TrkB signaling. Loss of TrkB in CST-expressing interneurons did not impact their survival or laminar distribution, nor did it alter intrinsic excitability or GABA release properties. However, loss of TrkB in CST-expressing cells decreased excitatory drive onto these cells, suggesting that BDNF-TrkB signaling in these interneurons is critical for establishment or maintenance of excitatory synaptic connections onto these cells. Together, the presented data support the hypothesia that the subpopulation of TrkB-expressing CST interneurons (~ 50% of all CST-expressing cells) constitute a set of cells that are critical for providing homeostatic inhibitory feedback in response to rising BDNF levels that promote neural excitation.

**Acknowledgements** We thank Dr. Daniel Weinberger and members of the Martinowich laboratory for critical reading of the manuscript.

**Funding** This work was supported by the National Institutes of Health (MH105592 to KM); the Epilepsy Foundation (Research Grant to KM); and the Lieber Institute for Brain Development.

## Compliance with ethical standards

**Conflict of interest** The authors declare that they have no conflict of interest.

**Ethical approval** All applicable international, national and/or institutional guidelines for the care and use of animals were followed.

## References

Aourz N, Portelli J, Coppens J, De Bundel D, Di Giovanni G, Van Eeckhaut A, Michotte Y, Smolders I (2014) Cortistatin-14 mediates its anticonvulsant effects via sst2 and sst3 but not ghrelin receptors. CNS Neurosci Ther 20(7):662–670

Baquet ZC, Gorski JA, Jones KR (2004) Early striatal dendrite deficits followed by neuron loss with advanced age in the absence of anterograde cortical brain-derived neurotrophic factor. J Neurosci 24(17):4250–4258

Binder DK, Routbort MJ, Ryan TE, Yancopoulos GD, McNamara JO (1999) Selective inhibition of kindling development by intraventricular administration of TrkB receptor body. J Neurosci 19(4):1424–1436

Bourgin P, Fabre V, Huitron-Resendiz S, Henriksen SJ, Prospero-Garcia O, Criado JR, de Lecea L (2007) Cortistatin promotes and negatively correlates with slow-wave sleep. Eur J Neurosci 26(3):729–738

Braun H, Schulz S, Becker A, Schroder H, Hollt V (1998) Protective effects of cortistatin (CST-14) against kainate-induced neurotoxicity in rat brain. Brain Res 803(1–2):54–60

Cellerino A, Maffei L, Domenici L (1996) The distribution of brain-derived neurotrophic factor and its receptor trkB in parvalbumin-containing neurons of the rat visual cortex. Eur J Neurosci 8(6):1190–1197

Chang J, Gilman SR, Chiang AH, Sanders SJ, Vitkup D (2015) Genotype to phenotype relationships in autism spectrum disorders. Nat Neurosci 18(2):191–198

de Lecea L (2008) Cortistatin–functions in the central nervous system. Mol Cell Endocrinol 286(1–2):88–95

de Lecea L, Criado JR, Prospero-Garcia O, Gautvik KM, Schweitzer P, Danielson PE, Dunlop CL, Siggins GR, Henriksen SJ, Sutcliffe JG (1996) A cortical neuropeptide with neuronal depressant and sleep-modulating properties. Nature 381(6579):242–245

de Lecea L, del Rio JA, Criado JR, Alcantara S, Morales M, Danielson PE, Henriksen SJ, Soriano E, Sutcliffe JG (1997) Cortistatin is expressed in a distinct subset of cortical interneurons. J Neurosci 17(15):5868–5880

Ding Y, Chang LC, Wang X, Guilloux JP, Parrish J, Oh H, French BJ, Lewis DA, Tseng GC, Sibille E (2015) Molecular and genetic characterization of depression: overlap with other psychiatric disorders and aging. Mol Neuropsychiatry 1(1):1–12

Ernfors P, Bengzon J, Kokaia Z, Persson H, Lindvall O (1991) Increased levels of messenger RNAs for neurotrophic factors in the brain during kindling epileptogenesis. Neuron 7(1):165–176

Estellar R, Echauz J, Tcheng T, Litt B, Pless B (2001) Line length: an efficient feature for seizure onset detection. Proceedings of the 23rd Annual International Conference of the IEEE

Faraguna U, Vyazovskiy VV, Nelson AB, Tononi G, Cirelli C (2008) A causal role for brain-derived neurotrophic factor in the homeostatic regulation of sleep. J Neurosci Official J Soc Neurosci 28:4088–4095

Fuchs T, Jefferson SJ, Hooper A, Yee PH, Maguire J, Luscher B (2017) Disinhibition of somatostatin-positive GABAergic interneurons results in an anxiolytic and antidepressant-like brain state. Mol Psychiatry 22(6):920–930

Gorba T, Wahle P (1999) Expression of TrkB and TrkC but not BDNF mRNA in neurochemically identified interneurons in rat visual cortex in vivo and in organotypic cultures. Eur J Neurosci 11(4):1179–1190

Grishanin RN, Yang H, Liu X, Donohue-Rolfe K, Nune GC, Zang K, Xu B, Duncan JL, Lavail MM, Copenhagen DR, Reichardt LF (2008) Retinal TrkB receptors regulate neural development in the inner, but not outer, retina. Mol Cell Neurosci 38(3):431–443

Guilloux JP, Douillard-Guilloux G, Kota R, Wang X, Gardier AM, Martinowich K, Tseng GC, Lewis DA, Sibille E (2012) Molecular evidence for BDNF- and GABA-related dysfunctions in the amygdala of female subjects with major depression. Mol Psychiatry 17(11):1130–1142

Hairston IS, Waxler E, Seng JS, Fezzey AG, Rosenblum KL, Muzik M (2011) The role of infant sleep in intergenerational transmission of trauma. Sleep 34(10):1373–1383

Heimel JA, van Versendaal D, Levelt CN (2011) The role of GABAergic inhibition in ocular dominance plasticity. Neural Plast 2011:391763

Hill JL, Hardy NF, Jimenez DV, Maynard KR, Kardian AS, Pollock CJ, Schloesser RJ, Martinowich K (2016) Loss of promoter IV-driven BDNF expression impacts oscillatory activity during sleep, sensory information processing and fear regulation. Transl Psychiatry 6(8):e873

Huang ZJ, Zeng H (2013) Genetic approaches to neural circuits in the mouse. Annu Rev Neurosci 36:183–215

Huang ZJ, Kirkwood A, Pizzorusso T, Porciatti V, Morales B, Bear MF, Maffei L, Tonegawa S (1999) BDNF regulates the maturation of inhibition and the critical period of plasticity in mouse visual cortex. Cell 98(6):739–755

Huber R, Deboer T, Tobler I (2000) Effects of sleep deprivation on sleep and sleep EEG in three mouse strains: empirical data and simulations. Brain Res 857(1–2):8–19

Huber R, Tononi G, Cirelli C (2007) Exploratory behavior, cortical BDNF expression, and sleep homeostasis. Sleep 30(2):129–139

Itami C, Kimura F, Nakamura S (2007) Brain-derived neurotrophic factor regulates the maturation of layer 4 fast-spiking cells after the second postnatal week in the developing barrel cortex. J Neurosci 27(9):2241–2252

Jacob J (2016) Cortical interneuron dysfunction in epilepsy associated with autism spectrum disorders. Epilepsia 57(2):182–193

Klaassen A, Glykys J, Maguire J, Labarca C, Mody I, Boulter J (2006) Seizures and enhanced cortical GABAergic inhibition in two mouse models of human autosomal dominant nocturnal frontal lobe epilepsy. Proc Natl Acad Sci USA 103(50):19152–19157

Koyama R, Ikegaya Y (2005) To BDNF or not to BDNF: that is the epileptic hippocampus. Neuroscientist 11(4):282–287

Lin LC, Sibille E (2015) Somatostatin, neuronal vulnerability and behavioral emotionality. Mol Psychiatry 20(3):377–387

Liu G, Kotloski RJ, McNamara JO (2014) Antiseizure effects of TrkB kinase inhibition. Epilepsia 55(8):1264–1273

Lucas EK, Jegarl A, Clem RL (2014) Mice lacking TrkB in parvalbumin-positive cells exhibit sexually dimorphicbehavioral phenotypes. Behav Brain Res 274:219–225. https://doi.org/10.1016/j.bbr.2014.08.011

Luttjohann A, Fabene PF, van Luijtelaar G (2009) A revised Racine's scale for PTZ-induced seizures in rats. Physiol Behav 98(5):579–586

Martinowich K, Schloesser RJ, Jimenez DV, Weinberger DR, Lu B (2011) Activity-dependent brain-derived neurotrophic factor expression regulates cortistatin-interneurons and sleep behavior. Mol Brain 4:11

Martinowich K, Cardinale KM, Schloesser RJ, Hsu M, Greig NH, Manji HK (2012) Acetylcholinesterase inhibition ameliorates deficits in motivational drive. Behav Brain Funct 8:15

Marty S, Berzaghi Mda P, Berninger B (1997) "Neurotrophins and activity-dependent plasticity of cortical interneurons". Trends Neurosci 20(5):198–202

Maynard KR, Hill JL, Calcaterra NE, Palko ME, Kardian A, Paredes D, Sukumar M, Adler BD, Jimenez DV, Schloesser RJ, Tessarollo L, Lu B, Martinowich K (2016) Functional role of BDNF production from unique promoters in aggression and serotonin signaling. Neuropsychopharmacology 41(8):1943–1955

McNamara JO, Scharfman HE (2012). Temporal Lobe Epilepsy and the BDNF Receptor, TrkB. Jasper's Basic Mechanisms of the Epilepsies. Noebels JL, Avoli M, Rogawski MA, Olsen RW and A. V. Delgado-Escueta. Bethesda (MD)

Merlio JP, Ernfors P, Kokaia Z, Middlemas DS, Bengzon J, Kokaia M, Smith ML, Siesjo BK, Hunter T, Lindvall O et al (1993) Increased production of the TrkB protein tyrosine kinase receptor after brain insults. Neuron 10(2):151–164

Moore EM, Boehm SL (2009) Site-specific microinjection of baclofen into the anterior ventral tegmental area reduces binge-like ethanol intake in male C57BL/6J mice. Behav Neurosci 123(3):555–563

Nagappan G, Lu B (2005) Activity-dependent modulation of the BDNF receptor TrkB: mechanisms and implications. Trends Neurosci 28(9):464–471

Nava C, Dalle C, Rastetter A, Striano P, de Kovel CG, Nabbout R, Cances C, Ville D, Brilstra EH, Gobbi G, Raffo E, Bouteiller D, Marie Y, Trouillard O, Robbiano A, Keren B, Agher D, Roze E, Lesage S, Nicolas A, Brice A, Baulac M, Vogt C, El Hajj N, Schneider E, Suls A, Weckhuysen S, Gormley P, Lehesjoki AE, De Jonghe P, Helbig I, Baulac S, Zara F, Koeleman BP, Euro ERESC, Haaf T, LeGuern E, Depienne C (2014) De novo mutations in HCN1 cause early infantile epileptic encephalopathy. Nat Genet 46(6):640–645

Paradiso B, Zucchini S, Su T, Bovolenta R, Berto E, Marconi P, Marzola A, Navarro Mora G, Fabene PF, Simonato M (2011) Localized overexpression of FGF-2 and BDNF in hippocampus reduces mossy fiber sprouting and spontaneous seizures up to 4 weeks after pilocarpine-induced status epilepticus. Epilepsia 52(3):572–578

Patterson PH (2011) Modeling autistic features in animals. Pediatr Res 69(5 Pt 2):34R–40R

Poolos NP (2012) Hyperpolarization-activated cyclic nucleotide-gated (HCN) ion channelopathy in epilepsy. Jasper's basic mechanisms of the epilepsies. th, Noebels JL, Avoli M et al. Bethesda (MD)

Price MG, Yoo JW, Burgess DL, Deng F, Hrachovy RA, Frost JD, Noebels JL (2009) A triplet repeat expansion genetic mouse model of infantile spasms syndrome, Arx(GCG)10 + 7, with interneuronopathy, spasms in infancy, persistent seizures, and adult cognitive and behavioral impairment. J Neurosci 29(27):8752–8763

Prince DA, Gu F, Parada I (2016) Antiepileptogenic repair of excitatory and inhibitory synaptic connectivity after neocortical trauma. Prog Brain Res 226:209–227

Reibel S, Depaulis A, Larmet Y (2001) BDNF and epilepsy–the bad could turn out to be good. Trends Neurosci 24(6):318–319

Rossignol E, Kruglikov I, van den Maagdenberg AM, Rudy B, Fishell G (2013) CaV 2.1 ablation in cortical interneurons selectively impairs fast-spiking basket cells and causes generalized seizures. Ann Neurol 74(2):209–222

Schweitzer P, Madamba SG, Siggins GR (2003) The sleep-modulating peptide cortistatin augments the h-current in hippocampal neurons. J Neurosci 23(34):10884–10891

Simonato M (2014) Gene therapy for epilepsy. Epilepsy Behav 38:125–130

Souza-Moreira L, Morell M, Delgado-Maroto V, Pedreno M, Martinez-Escudero L, Caro M, O'Valle F, Luque R, Gallo M, de Lecea L, Castano JP, Gonzalez-Rey E (2013) Paradoxical effect of cortistatin treatment and its deficiency on experimental autoimmune encephalomyelitis. J Immunol 191(5):2144–2154

Swanwick CC, Harrison MB, Kapur J (2004) Synaptic and extrasynaptic localization of brain-derived neurotrophic factor and the tyrosine kinase B receptor in cultured hippocampal neurons. J Comp Neurol 478(4):405–417

Taniguchi H, He M, Wu P, Kim S, Paik R, Sugino K, Kvitsiani D, Fu Y, Lu J, Lin Y, Miyoshi G, Shima Y, Fishell G, Nelson SB, Huang ZJ (2011) A resource of Cre driver lines for genetic targeting of GABAergic neurons in cerebral cortex. Neuron 71(6):995–1013

Thoby-Brisson M, Cauli B, Champagnat J, Fortin G, Katz DM (2003) Expression of functional tyrosine kinase B receptors by rhythmically active respiratory neurons in the pre-Botzinger complex of neonatal mice. J Neurosci 23(20):7685–7689

Timmusk T, Belluardo N, Persson H, Metsis M (1994) Developmental regulation of brain-derived neurotrophic factor messenger RNAs transcribed from different promoters in the rat brain. Neuroscience 60(2):287–291

Tononi G, Cirelli C (2014) Sleep and the price of plasticity: from synaptic and cellular homeostasis to memory consolidation and integration. Neuron 81(1):12–34

Weidner KL, Buenaventura DF, Chadman KK (2014) Mice overexpressing BDNF in forebrain neurons develop an altered behavioral phenotype with age. Behav Brain Res 268:222–228

Woo NH, Lu B (2006) Regulation of cortical interneurons by neurotrophins: from development to cognitive disorders. Neuroscientist 12(1):43–56

Xu X, Wells AB, O'Brien DR, Nehorai A, Dougherty JD (2014) Cell type-specific expression analysis to identify putative cellular mechanisms for neurogenetic disorders. J Neurosci 34(4):1420–1431